Commun. Comput. Phys.
doi: 10.4208/cicp.301011.310112s

Vol. **13**, No. 3, pp. 769-779
March 2013

Boundary Conditions for Combustion Field and LB Simulation of Diesel Particulate Filter

Kazuhiro Yamamoto*

Department of Mechanical Science and Engineering, Faculty of Engineering, Nagoya University, Furo-cho, Chikusa-ku, Nagoya, 464-8603 Japan.

Received 30 October 2011; Accepted (in revised version) 31 January 2012

Available online 29 August 2012

Abstract. A diesel particulate filter (DPF) is a key technology to meet future emission standards of particulate matters (PM), mainly soot. It is generally consists of a wall-flow type filter positioned in the exhaust stream of a diesel vehicle. It is difficult to simulate the thermal flow in DPF, because we need to consider the soot deposition and combustion in the complex geometry of filter wall. In our previous study, we proposed an approach for the conjugate simulation of gas-solid flow. That is, the gas phase was simulated by the lattice Boltzmann method (LBM), coupled with the equation of heat conduction inside the solid filter substrate. However, its numerical procedure was slightly complex. In this study, to reduce numerical costs, we have tested a new boundary condition with chemical equilibrium in soot combustion at the surface of filter substrate. Based on the soot oxidation rate with catalysts evaluated in experiments, the lattice Boltzmann simulation of soot combustion in the catalyzed DPF is firstly presented to consider the process in the after-treatment of diesel exhaust gas. The heat and mass transfer is shown to discuss the effect of catalysts.

AMS subject classifications: 76S05, 80A20, 80A25, 80A32

Key words: Lattice Boltzmann method, DPF, heat conduction, X-ray CT, multiphase flow.

1 Introduction

Although combustion is widely used in our society such as engines and practical combustors, the phenomena inside these applications are very complex, which depend upon interrelated processes of flow, heat and mass transfer, and chemical reactions [6]. Due to the recent progress of computers, a numerical simulation is a powerful means to model and predict various combustion phenomena.

*Corresponding author. *Email address:* kazuhiro@mech.nagoya-u.ac.jp (K. Yamamoto)

One of the important targets is to design a better internal combustion engine. For example, since diesel engines have an advantage of lower fuel consumption, compared with gasoline engines, it is possible to reduce CO_2 emission from transport industries such as passenger cars and cargo trucks. However, the emission of particulate matters (PM) including soot from diesel engines causes a severe environment problem. Recently, much attention worldwide has been given to the influence of fine particles in the atmosphere on human health [5]. Then, stricter exhaust emission standards such as Euro V in 2008 are being set in many countries.

A diesel particulate filter (DPF) is a key technology to meet future PM emission standards. It generally consists of a wall-flow type filter positioned in the exhaust stream of a diesel vehicle. Fig. 1 shows a cordierite filter used in this study. In simple explanation of DPF, it traps PM when exhaust gas passes through its porous wall (Fig. 1(b)). It is the most efficient after-treatment device. Latest our researches have shown that DPF filtration efficiency can be as high as 99 % [9]. The filter would be plugged with particles to cause an increase of filter back-pressure, which must be kept at lower levels, because the higher back-pressure increases fuel consumption and reduces available torque [8]. To prevent pressure build-up, the accumulated soot is removed from the filter by combustion [7], which is called filter regeneration process. Usually, the exhaust gas temperature is insufficient to regenerate the filter. The soot combustion (oxidation) temperature can be lowered by impregnation of the filter substrate with an oxidation catalyst.

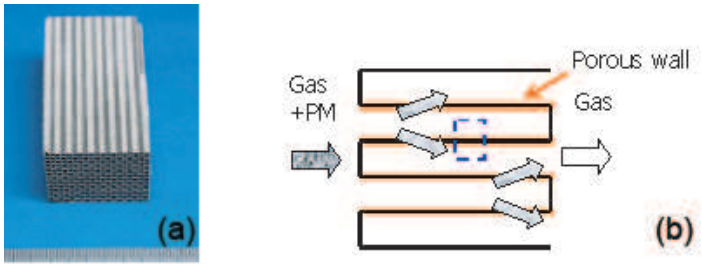

Figure 1: (a) Photograph of cordierite filter, and (b) PM trap inside porous filter wall. Calculation domain is shown by dotted line.

So far, there has not been enough data, and the phenomena occurring in the filter regeneration process are not well understood. This is because there are many difficulties in measurements. Typical inlet size of filter monolith is about 2 mm, and the thickness of the filter wall is only 0.2 mm where soot particles are removed. It is impossible to observe the small-scale phenomena inside the filter experimentally.

In this study, we firstly simulate the flow in a real catalyzed DPF by the lattice Boltzmann method (LBM). The structure of a cordierite filter is scanned by a 3D X-ray CT (Computed Tomography) technique. By conducting tomography-assisted simulation, it is possible to discuss the soot oxidation with catalyst, which is hardly obtained by measurements. Especially, to reduce numerical costs, we test a new boundary condition with chemical equilibrium. The lattice Boltzmann simulation of soot combustion in DPF is

presented to consider the process in the after-treatment of diesel exhaust gas. The heat and mass transfer is shown to discuss the effect of catalysts.

2 Numerical approach

2.1 Lattice Boltzmann method

To simulate the flow in the gas phase, we use the lattice Boltzmann method (LBM). The fundamental idea of LBM is to construct simplified kinetic models that incorporate the essential physics of microscopic or mesoscopic processes so that the macroscopic averaged properties obey the desired macroscopic equations such as the N-S equations. The kinetic equation provides any of the advantages of molecular dynamics, including clear physical pictures, easy implementation of boundary conditions, and fully parallel algorisms [1]. LBM fulfills these requirements in a straightforward manner. So far, many benchmark studies have been conducted [2, 10–12, 15].

Here, we explain the numerical procedure [13–16]. The flow is described by the lattice BGK equation in terms of the distribution function. The evolution equation using the pressure distribution function is

$$p_\alpha(\boldsymbol{x}+\boldsymbol{c}_\alpha\delta_t,t+\delta_t)-p_\alpha(\boldsymbol{x},t)=-\frac{1}{\tau}\left[p_\alpha(\boldsymbol{x},t)-p_\alpha^{eq}(\boldsymbol{x},t)\right], \tag{2.1}$$

where $c=\delta_x/\delta_t$, and δ_x and δ_t are the lattice constant and the time step, and τ is the relaxation time that controls the rate of approach to equilibrium. The equilibrium distribution function, p_α^{eq}, is given by

$$p_\alpha^{eq}=w_\alpha\left(p+p_0\left(3\frac{(\boldsymbol{c}_\alpha\cdot\boldsymbol{u})}{c^2}+\frac{9}{2}\frac{(\boldsymbol{c}_\alpha\cdot\boldsymbol{u})^2}{c^4}-\frac{3}{2}\frac{\boldsymbol{u}\cdot\boldsymbol{u}}{c^2}\right)\right). \tag{2.2}$$

The sound speed, c_s, is $c/\sqrt{3}$ with $p_0=\rho_0RT_0=\rho_0c_s^2$. Here, p_0 and ρ_0 are the pressure and density in the reference conditions. In this study, 2D simulation is conducted by D2Q9 model. The pressure and local velocity of $\boldsymbol{u}=(u_x,u_y)$ are obtained using the ideal gas equation

$$p=\sum_\alpha p_\alpha, \tag{2.3a}$$

$$u=\frac{\rho_0}{\rho}\frac{1}{p_0}\sum_\alpha\boldsymbol{c}_\alpha p_\alpha=\frac{T}{T_0}\frac{1}{p_0}\sum_\alpha\boldsymbol{c}_\alpha p_\alpha. \tag{2.3b}$$

To consider the variable density, we adopt the low Mach number approximation. The relaxation time is related with transport coefficients such as kinetic viscosity using $\nu=(2\tau-1)/6c^2\delta_t$. Through the Chapman-Enskog procedure, the Navier-Stokes equations

are derived from these equations [1]. The LBM formula for temperature and concentration fields is

$$F_{s,\alpha}(\boldsymbol{x}+\boldsymbol{c}_\alpha\delta_t,t+\delta_t)-F_{s,\alpha}(\boldsymbol{x},t)=-\frac{1}{\tau_s}\left[F_{s,\alpha}(\boldsymbol{x},t)-F^{eq}_{s,\alpha}(\boldsymbol{x},t)\right]+w_\alpha Q_s,\quad s=T,Y_i, \tag{2.4}$$

where Q_s is the source term due to chemical reaction. The equilibrium distribution function, $F^{eq}_{s,\alpha}$, is

$$F^{eq}_{s,\alpha}=w_\alpha\cdot s\left(1+3\frac{(\boldsymbol{c}_\alpha\cdot\boldsymbol{u})}{c^2}+\frac{9}{2}\frac{(\boldsymbol{c}_\alpha\cdot\boldsymbol{u})^2}{c^4}-\frac{3}{2}\frac{\boldsymbol{u}\cdot\boldsymbol{u}}{c^2}\right). \tag{2.5}$$

Temperature, T, and mass fraction of species, Y_i, are determined by these distribution functions:

$$T=\sum_\alpha F_{T,\alpha}, \tag{2.6a}$$

$$Y_i=\sum_\alpha F_{Y_i,\alpha}. \tag{2.6b}$$

In the process of after-treatment with catalyzed DPF, the following three processes are included: (a) soot is reacted with oxygen in gas phase; (b) the unburned soot in the first process is deposited onto the surface of filter substrate; and (c) the deposited soot burns on the catalyst. The deposition process of soot particles is explained by the Brownian diffusion, interception, inertial impaction, and gravity. When the actual size of PM is taken into consideration, the analysis must be performed on the nanometer-scale and, consequently, a large computational cost will be needed for the calculation. Therefore, it is impractical to consider the complex geometry of nano-sized soot particles. Instead, the soot concentration is monitored on the surface of the filter substrate or the soot layer [16]. The mass fraction of deposited soot is given by

$$Y_{C,surface}(\boldsymbol{x},t+\delta_t)=\sum_\alpha F_{C,\alpha}(\boldsymbol{x},t)\cdot P_D+Y_{C,surface}(\boldsymbol{x},t), \tag{2.7}$$

where $Y_{C,surface}$ is the mass fraction of soot on the filter substrate or the deposited soot layer at each time step. It is noted that P_D is the soot deposition probability. Soot at P_D is deposited, whereas soot at $(1-P_D)$ is not deposited and is bounced back into the flow. Exfoliation of the soot layer, due to the flow, is not taken into consideration. The value of P_D is determined by the same procedure of our previous experiments [16]. In this study, P_D is 0.002.

Expectedly, $Y_{C,surface}$ is increased when the soot in gas phase accumulates on the surface of filter substrate. As the soot deposition continues, the soot concentration sometime becomes unity. When this limit is reached, the solid site is piled up. The deposited soot region is treated as a non-slip wall, which implies a dynamic change in the boundary condition for the fluid. In this way, the soot deposition layer grows. In the process of after-treatment with catalyzed DPF, both the soot oxidation and the soot deposition are taken into consideration. In the present simulation, the soot oxidation in gas phase was set as a one-step irreversible reaction, proposed by our previous study [14].

2.2 Heat transfer in solid phase

In the after-treatment of diesel exhaust gas, the gas phase temperature due to soot combustion becomes high to cause the heat transfer to the solid phase of filter substrate. Then, the following equation of heat conduction is solved [12]

$$\frac{\partial T}{\partial t}=\frac{\lambda}{\rho_s C_p}\left(\frac{\partial^2 T}{\partial x^2}+\frac{\partial^2 T}{\partial y^2}\right), \tag{2.8}$$

where λ, ρ_s and C_p are the heat conductivity, density, and heat capacity of the filter. These values of the cordierite filter are 1.9 W/mK, 2500 kg/m^3, and 1170 J/kgK. Needless to say, any terms of convection and chemical reaction are not included in this equation. By coupling the equations in gas phase and using appropriate boundary conditions, it is possible to solve the problem. In order to determine the temperature at the interface between gas and solid phases, it is assumed that the temperature and heat flux in the gas phase are equal to those in solid phase. Other boundary conditions are explained in the next section.

2.3 Calculation domain and X-ray CT technique

To simulate the flow in the real diesel filter, we obtain the inner structure of filter wall by the 3D X-ray CT technique [13–16]. Non-destructive nature of the CT technique allows flow visualization of filter wall actually used. We have confirmed the applicability of the tomography-assisted simulation of DPF. In the present study, we employ a similar data processing technique.

Fig. 2 shows a CT image of the filter. Three slice images of the filter wall are shown. The spatial resolution is 1.15 μm/pix, which is the finest level in the reported CT measurements. The image area is 284 μm(x) $\times$ 661 μm(y) $\times$ 661 μm(z), and the grid number is 380 (x) $\times$ 576 (y) $\times$ 576 (z). The exhaust gas passes through the filter wall in the x-direction. Complex porous structure with variety of pore size is well observed. The averaged porosity of the filter wall is about 0.59. In the simulation, the two-dimensional slice image in x-y plane is used.

We add inlet and outlet zones of 23 μm (20 grids) in x-direction. Then, the calculation domain in the present 2D simulation is 330 μm $\times$115 μm, which is the sum of filter thickness and inlet and outlet zones. The grid number is 290 (N_x)$\times$101 (N_y). The grid size is 1.15 μm, which is the spatial resolution in X-ray CT measurement. As for the boundary condition, the inflow boundary is adopted at the inlet [2]. The inlet velocity of U_{in} is 0.1 m/s. The gas component is of the diesel exhaust gas, and the oxygen concentration in volume is 10 %. Its temperature is 673 K [14], and the soot mass fraction is 0.01. At the sidewall, the slip boundary conditions are adopted, considering the symmetry [4]. At the outlet, the pressure is constant, and the gradient of scalar such as temperature and mass fraction is set to be zero. On the surface of filter substrate, a non-slip boundary condition is adopted [3].

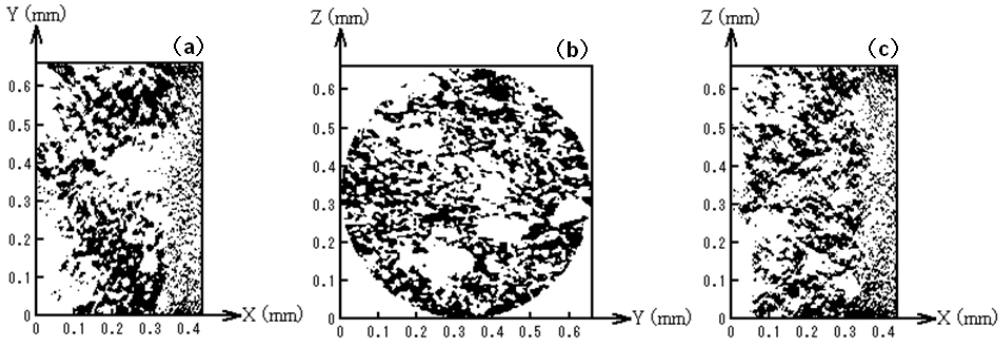

Figure 2: CT image of cordierite DPF is shown; (a) xy plane, (b) yz plane, and (c) xz plane.

3 Results and discussion

3.1 Estimation of soot oxidation rate with catalyst

First, the reaction rate of soot oxidation with catalyst is estimated. Since there is enough oxygen to oxidize the soot in diesel exhaust gas, it can be assumed that the reaction rate is expressed by the reaction rate constant, k, and the soot mass fraction, Y_{soot}:

$$\frac{\partial Y_{soot}}{\partial t} = kY_{soot}, \tag{3.1a}$$

$$k = A\exp(-\frac{E}{RT}). \tag{3.1b}$$

Then, by plotting the mass of oxidized soot in the form of natural logarithm of the Arrhenius equation, reaction constants of Arrhenius factor, A, and activation energy, E, can be determined. The result in an engine test [9] is shown in Fig. 3. The obtained values are $A = 5.92\times10^9$ 1/s, $E = 184$ kJ/mol.

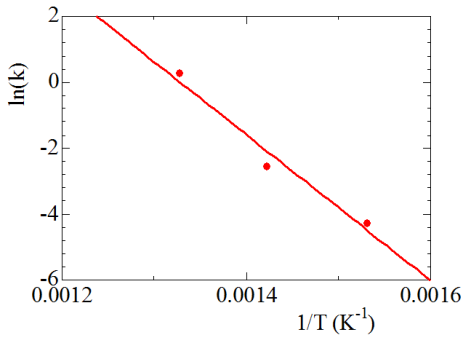

Figure 3: Arrhenius plot to estimate reaction constants of Arrhenius factor, A, and activation energy, E.

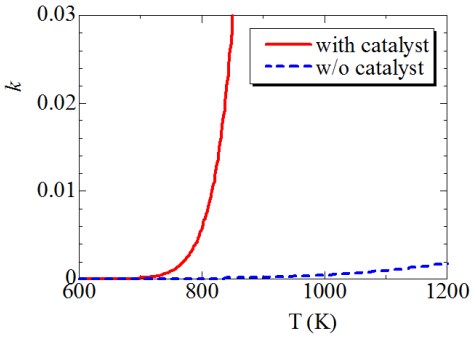

Figure 4: Reaction rate constants with and without catalyst.

It is well-known that the catalyst reduces the activation energy and promotes the chemical reaction. To make clear the effect of catalyst, the reaction rate constants with and without catalyst are compared. The reaction rate constant without catalyst is the value of gas phase reaction [14]. The obtained reaction rate constant, k, is shown in Fig. 4. The value with catalyst is much larger than that without catalyst. It is found that, above 700 K, the reaction rate constant is largely increased. That is, the soot oxidation is much promoted in this temperature range.

3.2 Soot oxidation in DPF

The soot oxidation process in DPF is simulated. Fig. 5 shows the time-variation of temperature profile. Time, t, is counted after we start the simulation. It is found that, at the beginning, only the temperature of gas phase is increased due to the soot oxidation. Then, the filter substrate of solid phase is heated. To discuss the process of after-treatment with catalyst, the simulation is continued until the steady state is achieved.

Fig. 6 shows the distributions of flow field, mass fraction of soot and oxygen, and reaction rate. The steady state is observed at t = 200 ms. As seen in Fig. 6(a), the exhaust gas is forced to pass through the narrow tunnel in pore structure of the filter. At the same time, the pressure is gradually decreased along the flow direction. On the other hand, as shown in Fig. 5(c), the temperatures of gas phase and solid phase are almost uniform. The soot concentration is decreased very quickly. Interestingly, in some area, the oxygen is not consumed, because this region is isolated, and oxygen cannot be reacted with soot. At the filter exit, the soot concentration is completely zero. That is, the after-treatment of exhaust gas is complete. Needless to say, the reaction rate locally varies, simply because the mass transfer of these reactants is different. However, the reaction rate on the surface of filter substrate is very high. Therefore, the soot oxidation is largely promoted by the catalyst, and resultantly, the soot deposition region is not observed. Then, at this condition, the continuously regenerating trap is achieved, where the filter could not be plugged with deposited soot.

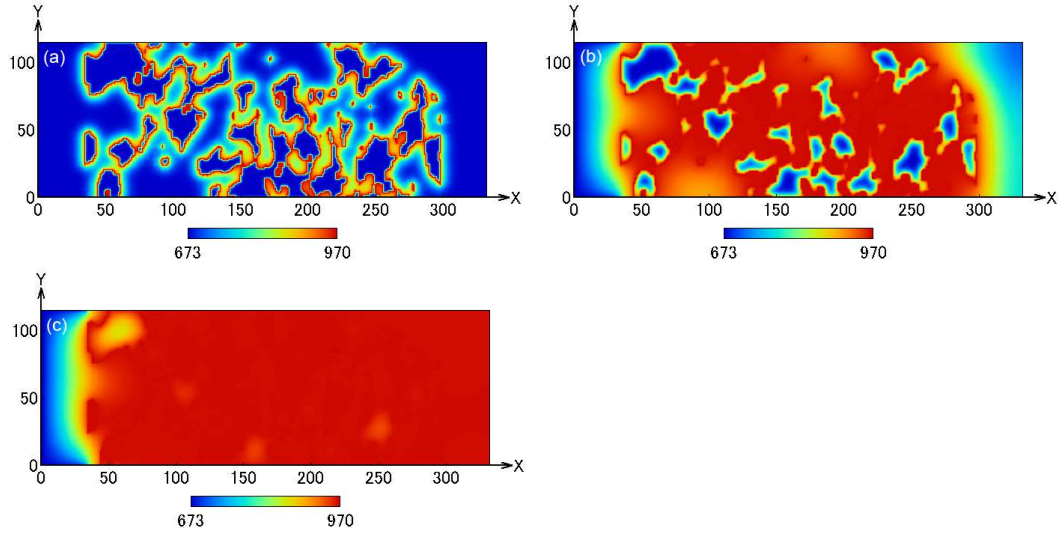

Figure 5: Time-variation of temperature profile; (a) $t = 0.23$ms, (b) $t = 6.9$ms, and (c) $t = 115$ms. It is observed that temperature only in gas phase is increased at the beginning.

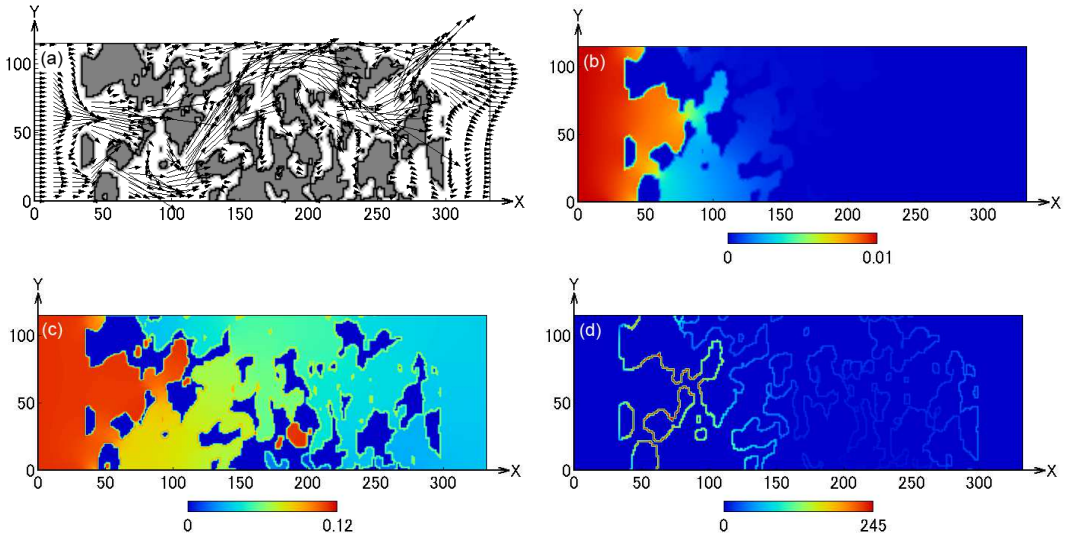

Figure 6: Profiles of (a) flow field, (b) mass fraction of soot, (c) mass fraction of oxygen, and (d) reaction rate. These are obtained under steady state. It is observed that soot oxidation is largely promoted by catalyst.

Next, we examine the time-variation of temperatures of gas and solid phases, which is shown in Fig. 7. To make clear the temperature rise inside the filter wall, the averaged values of both phases are calculated. At the beginning, only the temperature of gas phase is increased, because the soot oxidation is an exothermic reaction. Then, the filter substrate of solid phase is heated by the heat transfer from the gas phase to the solid phase. Although both temperatures are finally saturated to be the adiabatic temperature [6], the

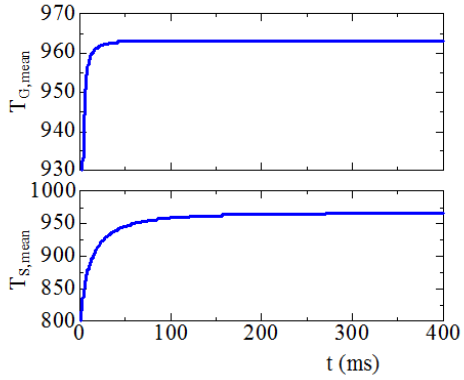

Figure 7: Time-variation of temperatures in gas and solid phases.

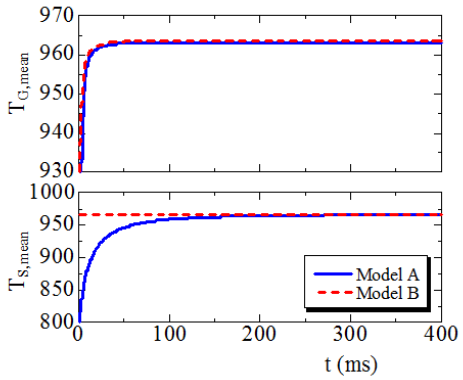

Figure 8: Time-variation of temperatures in gas and solid phases predicted by model A and model B.

time variation is different. Apparently, this tendency is explained by the fact that the heat capacity between gas phase and solid phase is largely different.

As explained in Section 2.2, in addition to the simulation of gas phase by LBM, we solve the equation of heat conduction of solid phase. However, as described above, under steady state, both temperatures are very close to the adiabatic temperature (T_{ad}) with chemical equilibrium. Then, a new boundary condition is tested. That is, at the filter substrate, we set the temperature of T_{ad}, which can reduce numerical costs. In this study, the original model by solving the equation of heat conduction is called model A. The alternate model with boundary condition with T_{ad} at the filter substrate is called model B, where the temperature of solid phase is set to be the equilibrium value of T_{ad}. The comparison between two models is shown in Fig. 8. As for the gas phase temperature, a good agreement is observed. That is, the average temperature in the gas phase is well predicted by model B. This may be because the soot concentration in the exhaust gas is constant and the soot oxidation occurs mainly on the catalyst, where the temperature is increased to be the adiabatic temperature.

In model B, we did not have to solve the area inside the filter substrate of solid wall. Since the porosity of the filter is about 60 %, and that area is 40 %. Then, in the present simulation, by comparing with model A, the calculation time of model B was reduced only by 5 %, which may depend on the simulation region. However, the boundary condition is simple and the program code can be less. Therefore, the model B by setting the solid wall with T_{ad} could be useful.

4 Conclusions

We have conducted the lattice Boltzmann simulation of exhaust gas flow by coupling with the equation of heat conduction to consider the soot combustion and heat transfer

in DPF. At filter substrate, the new boundary condition with adiabatic temperature (T_{ad}) of chemical equilibrium was tested to reduce numerical costs. The following results are obtained:

1. In experiments, the soot oxidation rate with catalyst was evaluated, and Arrhenius kinetic coefficients were determined. The estimated values of Arrhenius factor and activation energy are $A = 5.92 \times 10^9$ 1/s and E = 184 kJ/mol. Soot oxidation is much promoted when the temperature is higher than 700 K.
2. At the filter exit, the soot concentration is completely zero. Since the reaction rate on the surface of filter substrate is very high, the soot is fully oxidized inside the DPF. Therefore, the soot oxidation is largely promoted by the catalyst, and the soot layer formed by deposited soot is not observed. At this condition, the continuously regenerating trap is achieved.
3. Based on the time-variation of temperatures of gas and solid phases, the gas phase temperature is firstly increased due to the soot oxidation. Then, the filter substrate of solid phase is heated by the heat transfer from the gas phase to the solid phase. Under steady state, temperatures of gas and solid phases are almost equal to T_{ad}. Resultantly, the temperature field is well predicted by model B, where the equation of heat conduction is not solved and the temperature is assumed to be T_{ad} at filter substrate, which reduces numerical costs.

Acknowledgments

This work was partially supported by the Rare Metal Substitute Materials Development Project of New Energy and Industry Technology Development Organization (NEDO) in Japan.

References

[1] S. Chen and G. D. Doolen, Lattice Boltzmann method for fluid flows, Annu. Rev. Fluid Mech., 30 (1998), 329-364.
[2] X. He, S. Chen, and G. D. Doolen, A novel thermal model for the lattice Boltzmann method in incompressible limit, J. Comp. Phys., 146 (1998), 282-300.
[3] X. He and Li-Shi Luo, Lattice Boltzmann model for the incompressible Navier-Stokes equation, J. Stat. Phys., 88 (1997), 927-944.
[4] T. Inamuro, M. Yoshino, and F. Ogino, Lattice Boltzmann simulation of flows in a three-dimensional porous structure, Int. J. Numer. Meth. Fluids, 29 (1999), 737-748.
[5] D. B. Kittelson, Engines and nanoparticles: a review, J. Aerosol Sci., 29 (1998), 575-588.
[6] K. K. Kuo, Principles of Combustion, John Wiley & Sons, New York, 1986.
[7] G. Neri, L. Bonaccorsi et al., Catalytic combustion of diesel soot over metal oxide catalysts, Applied Catalysis B: Environmental, 11 (1997), 217-231.
[8] A. M. Stamatelos, A review of the effect of particulate traps on the efficiency of vehicle diesel engines, Energy Conversion and Management, 38(1) (1997), 83-99.

[9] K. Tsuneyoshi, O. Takagi, and K. Yamamoto, Effects of washcoat on initial PM filtration efficiency and pressure drop in SiC DPF, SAE 2011 World Congress 2011-01-0817, 2011, pp. 297-305.
[10] K. Yamamoto, LB simulation on combustion with turbulence, International Journal of Modern Physics B, 17(1/2) (2003), 197-200.
[11] K. Yamamoto, X. He, and G. D. Doolen, Simulation of combustion field with lattice Boltzmann method, J. Stat. Phys., 107 (2002), 367-383.
[12] K. Yamamoto and M. Nakamura, Simulation on flow and heat transfer in diesel particulate filter, ASME Journal of Heat Transfer, 133(6) (2011), 060901.
[13] K. Yamamoto, M. Nakamura, H. Yane, and H. Yamashita, Simulation on catalytic reaction in diesel particulate filter, Catalysis Today, 153 (2010), 118-124.
[14] K. Yamamoto, S. Oohori, H. Yamashita, and S. Daido, Simulation on soot deposition and combustion in diesel particulate filter, Proceeding of the Combustion Institute, 32, 2009, pp. 1965-1972.
[15] K. Yamamoto, S. Satake, H. Yamashita, N. Takada, and M. Misawa, Lattice Boltzmann simulation on porous structure and soot accumulation, Mathematics and Computers in Simulation, 72 (2006), 257-263.
[16] K. Yamamoto, K. Yamauchi, N. Takada, M. Misawa, H. Furutani, and O. Shinozaki, Lattice Boltzmann simulation on continuously regenerating diesel filter, Philosophical Transactions A (The Royal Society, London), 369 (2011), 2584-2591.